Synthesis and characterization of nickel (II) homogenous and supported complexes for the hydrogenation of furfural to furfuryl alcohol

Menala Kalumpha[1*], Leah. C. Matsinha[1], Banothile. C. E. Makhubela[1]

[1]*Research Center for Synthesis and Catalysis, Department of Chemical Sciences, University of Johannesburg, Auckland Park 2006, Johannesburg-South Africa.*

Supplementary Information

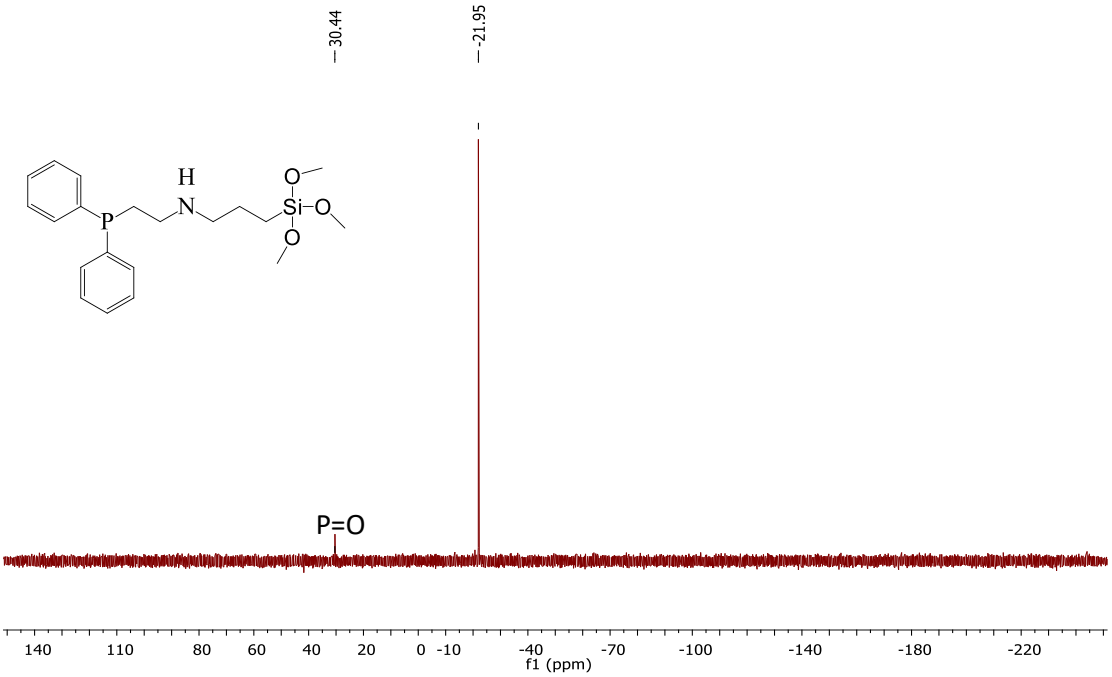

Figure S1 $^{31}P\{^{1}H\}$ NMR spectrum for ligand **L1** in $CDCl_3$ (500 MHz).

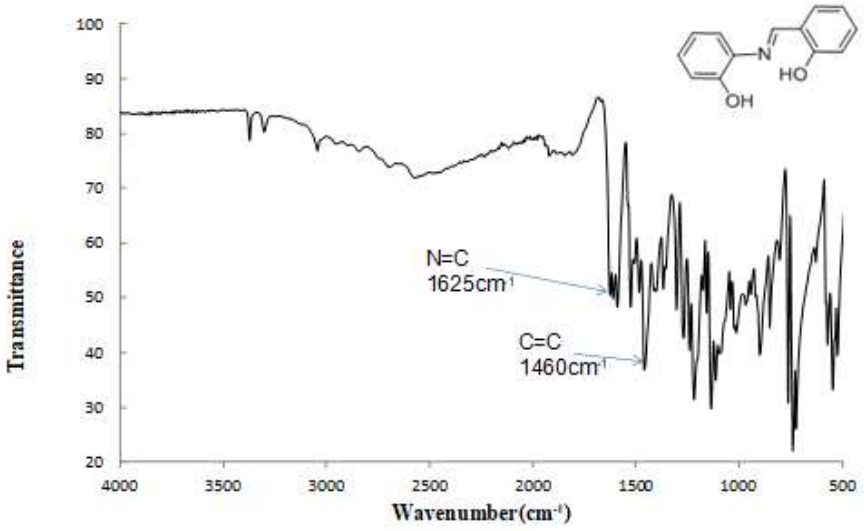

Figure S2 Infrared spectrum of ligand **L2.**

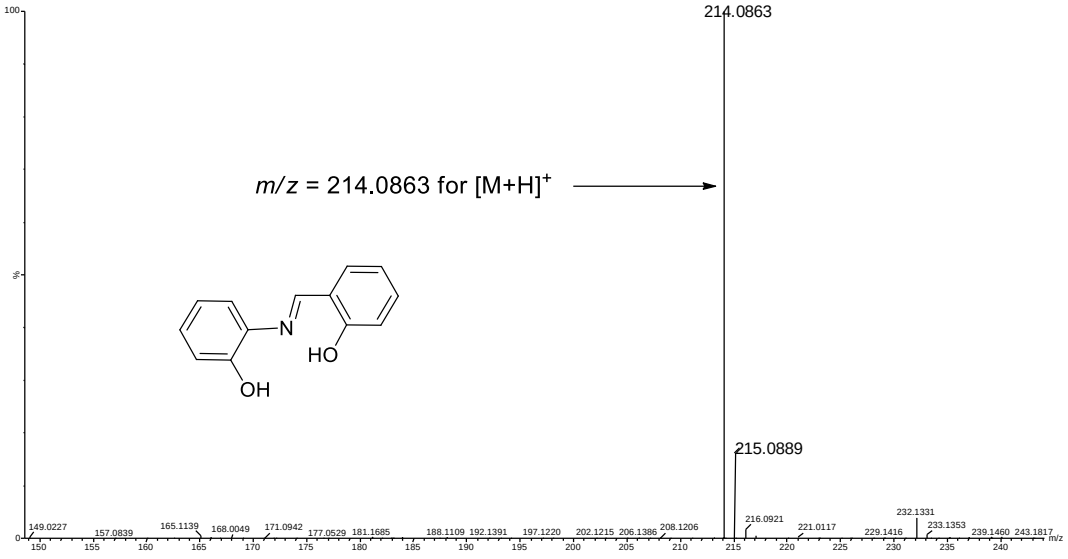

Figure SI 2b. Mass spectrum of L2.

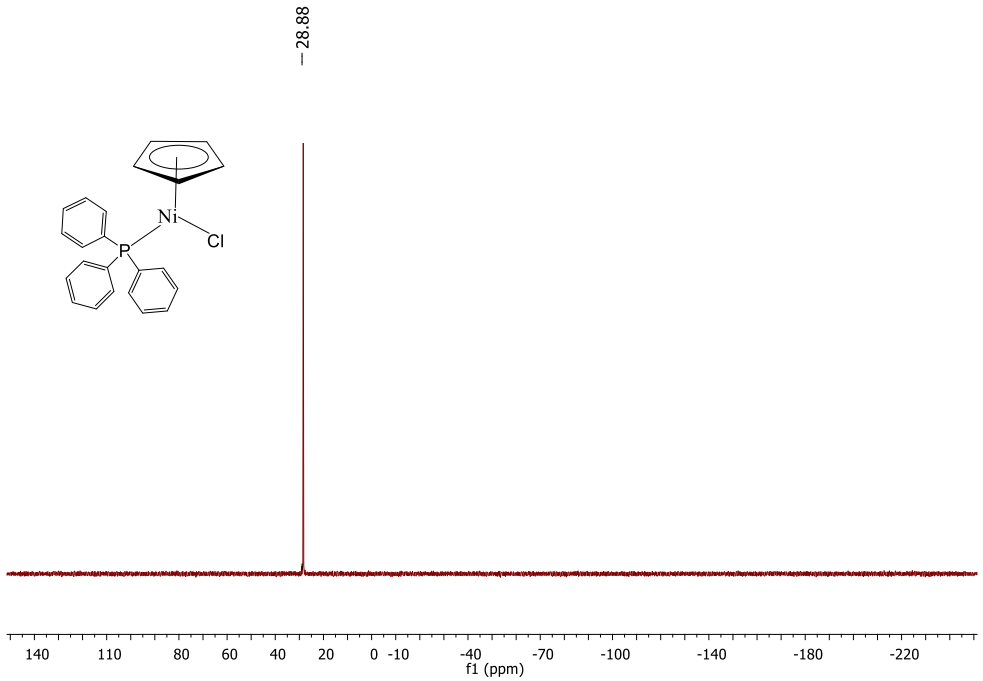

Figure S3 $^{31}P\{^{1}H\}$ NMR of complex **C1** in $CDCl_3$ (500 MHz).

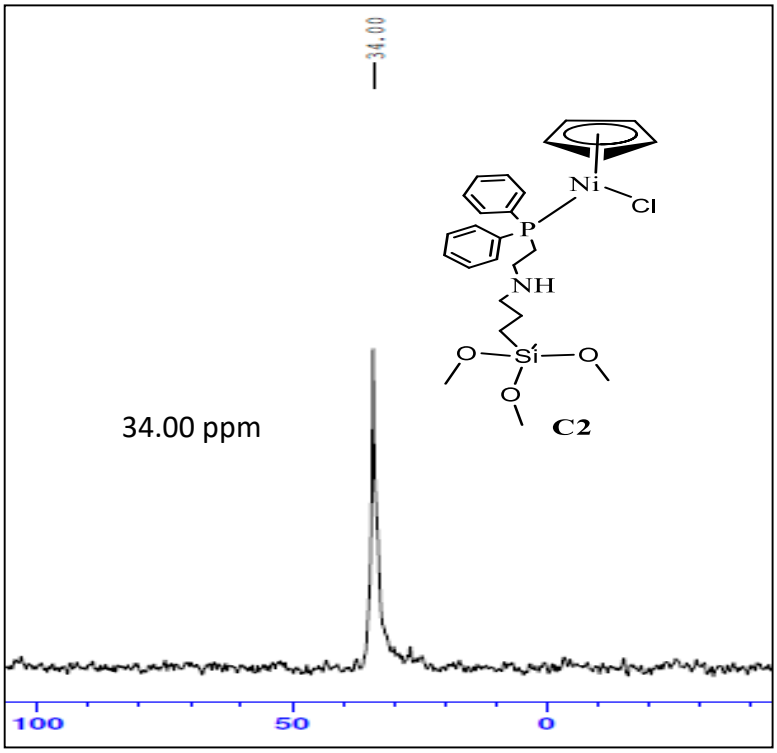

Figure S4 $^{31}P\{^{1}H\}$ NMR spectrum of complex **C2** in $CDCl_3$ (500 MHz).

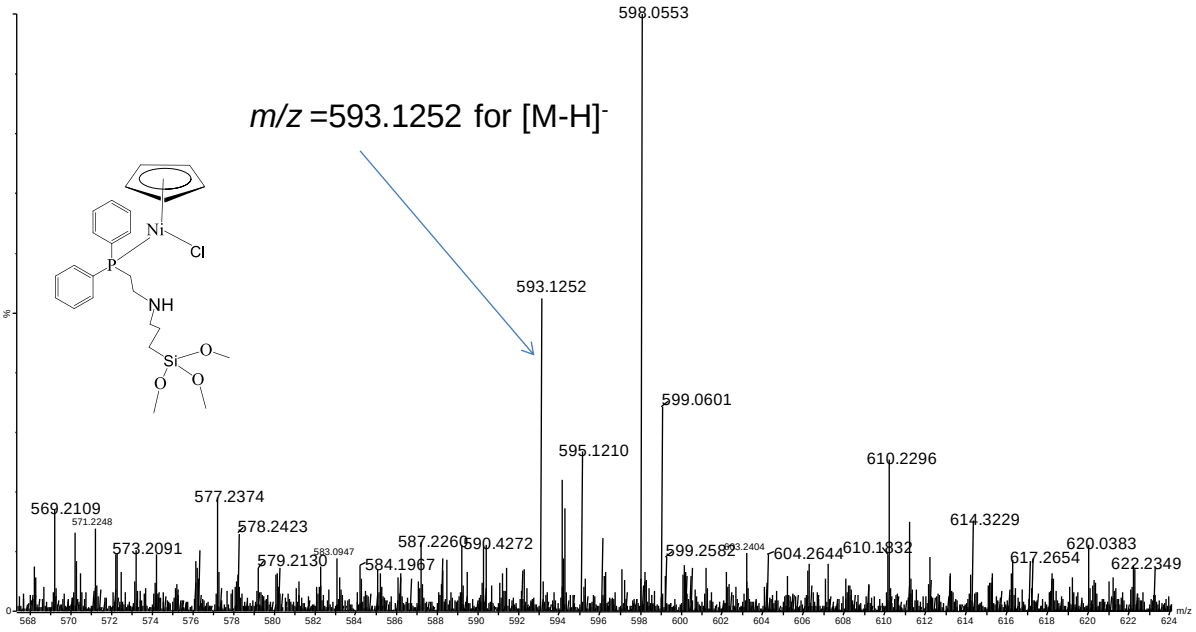

Figure S5 Mass spectrum of complex **C2.**

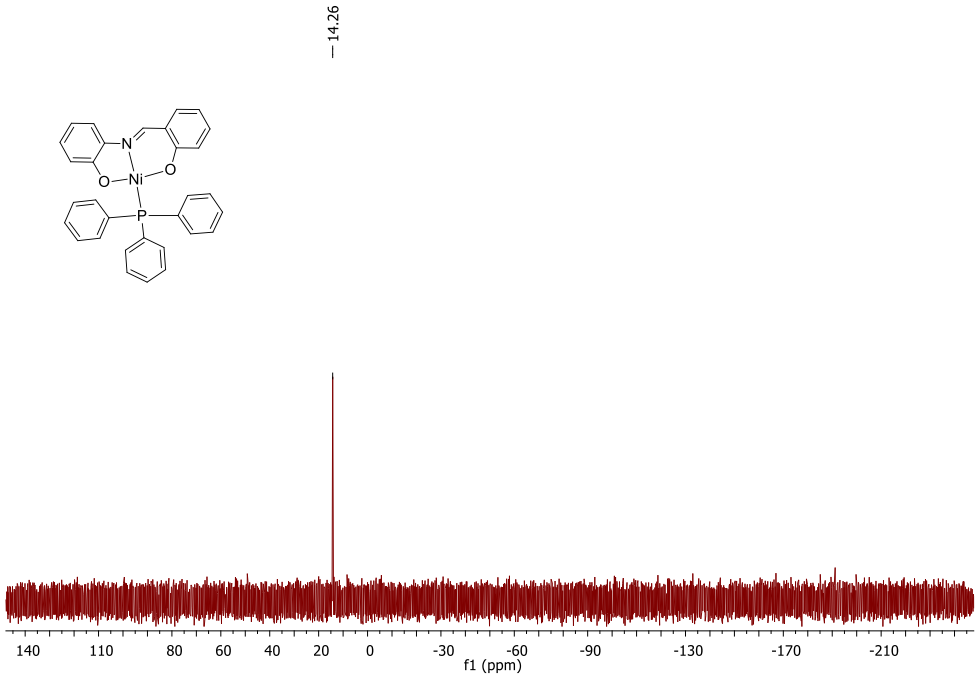

Figure S6 $^{31}P\{^{1}H\}$ NMR for complex **C4** in $CDCl_3$ (500 MHz)

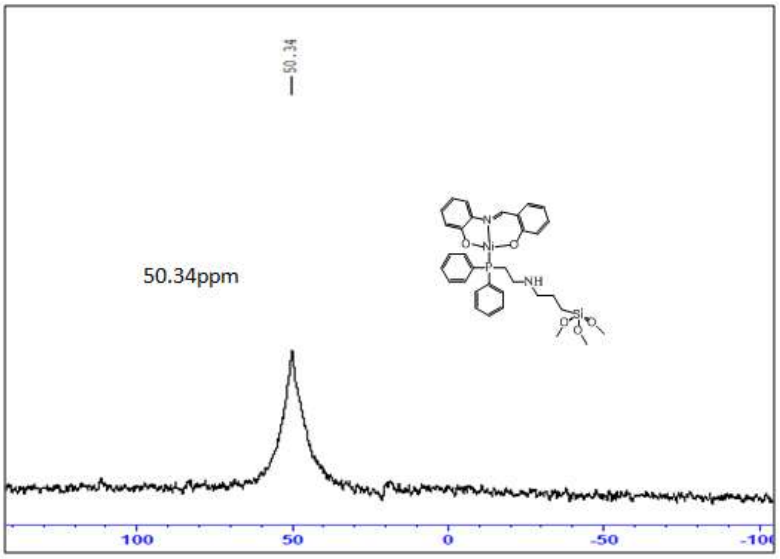

Figure S7 $^{31}P\{^{1}H\}$ NMR spectrum of complex **C5**

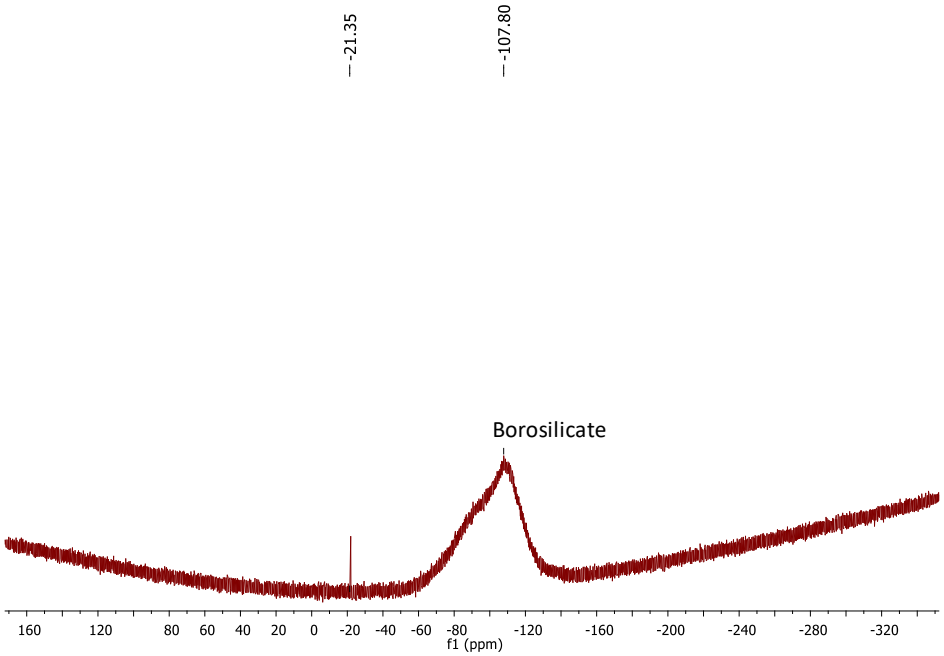

Figure S8 ^{29}Si NMR spectrum of complex **C5**

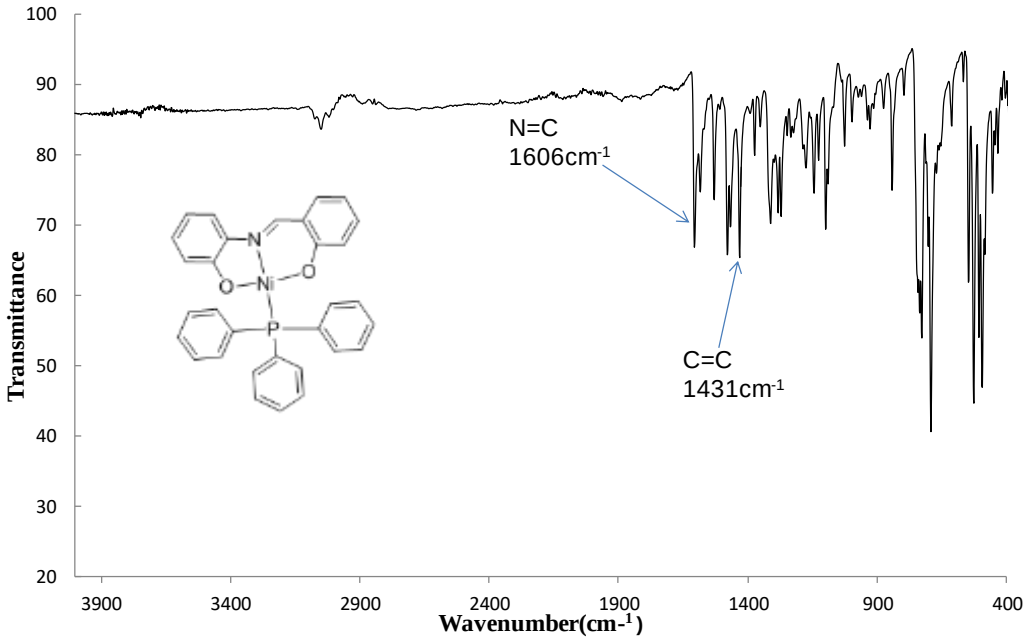

Figure S9 IR spectrum of complex **C4**

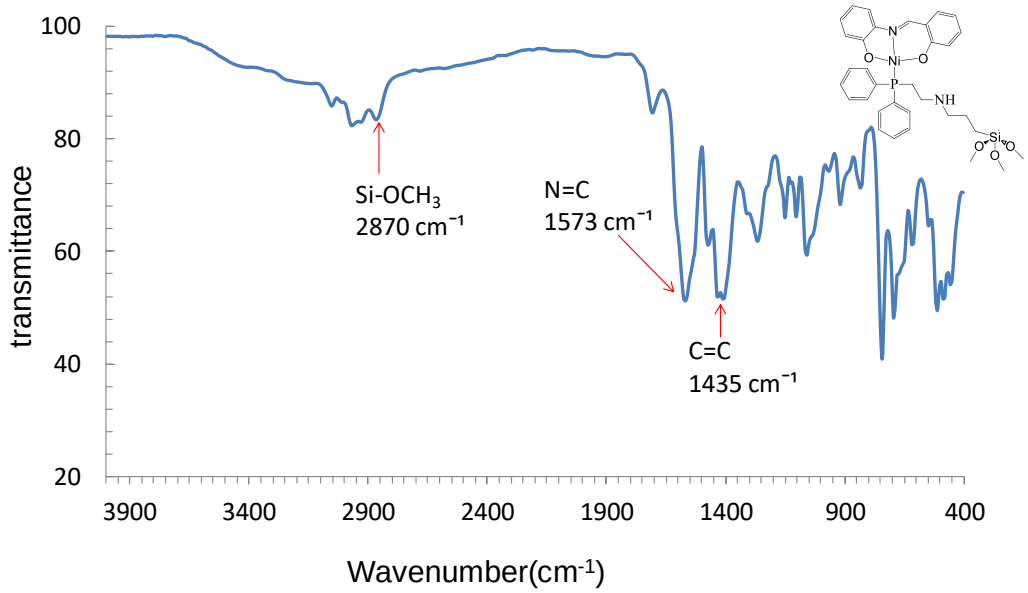

Figure S10 Infrared spectrum of complex **C5.**

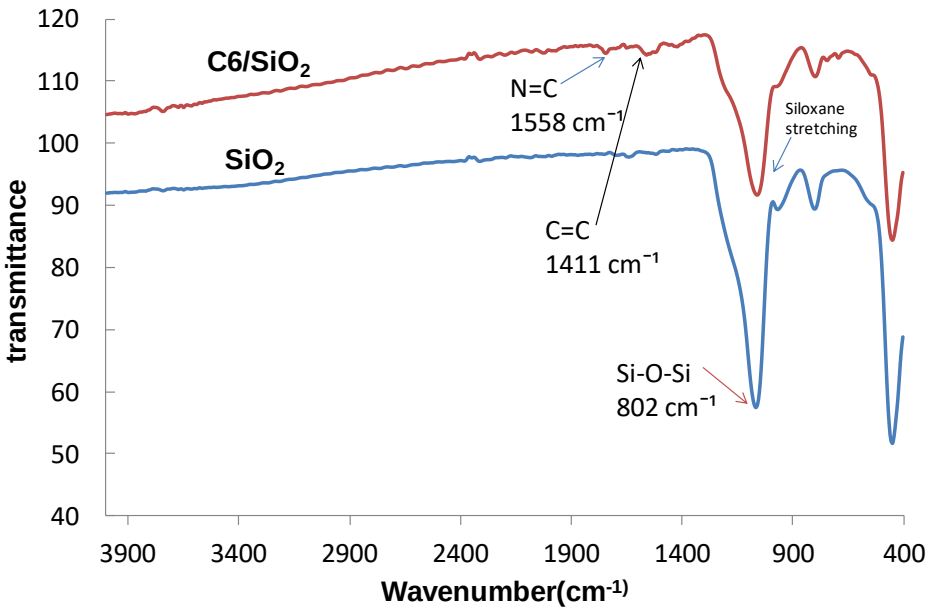

Figure S11 FT-IR spectra of silica gel (bottom), supported schiff base complex **C6** (top).

Table S1. The surface properties of silica gel and Ni (II) anchored catalysts **C3** and **C6**

Entry	Catalyst	S_{BET} (m^2/g)	Vp (cm^3/g)	Dp (nm)
1	SiO2	442	0.69	5.13
2	$C3/SiO_2$	258	0.39	4.63
3	$C6/SiO_2$	185	0.27	4.21

S_{BET} (BET specific surface area), Vp (pore volume), Dp (pore diameter)

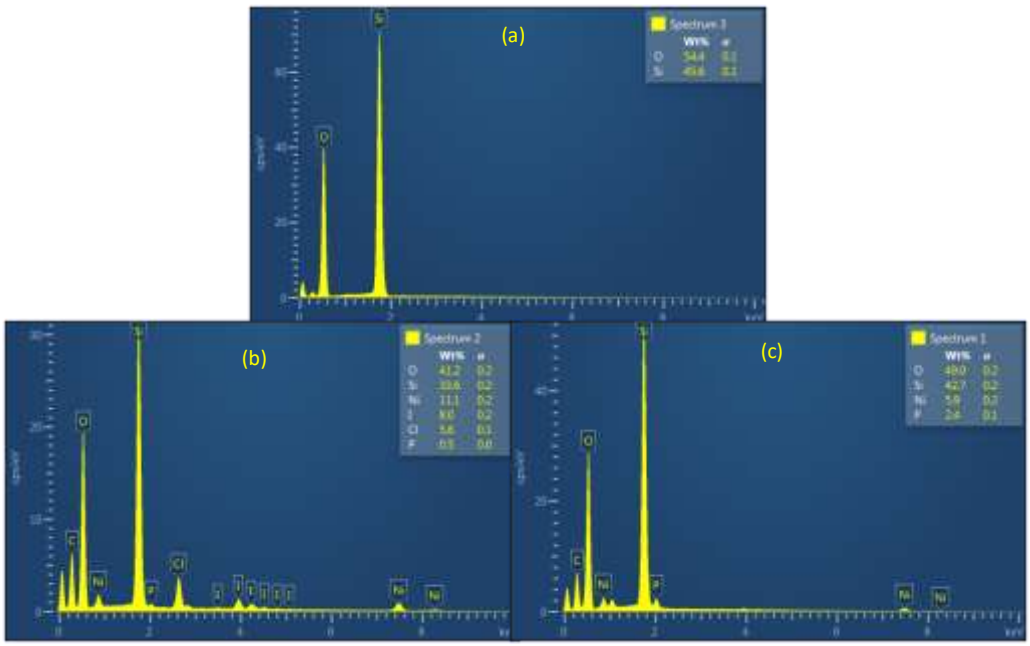

Figure S12. EDX images of silica gel (a), Ni (II) supported half-sandwich complex **C3** (b) and schiff base complex **C6** (c).

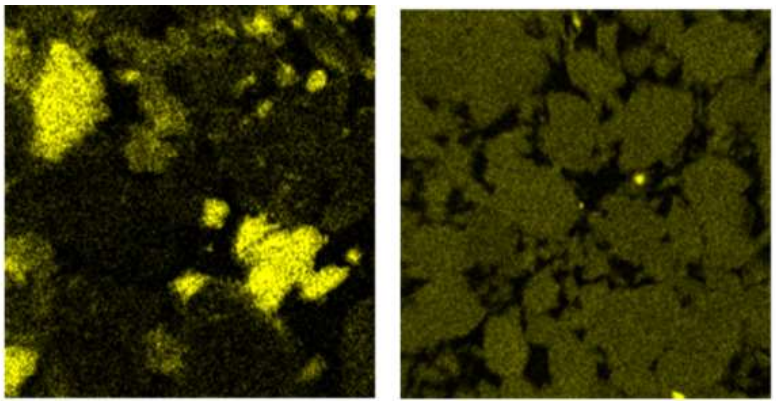

Figure S13 EDX images showing Ni mapping on the supported half-sandwich complex **C3** (a) and Schiff base complex **C6** (b).

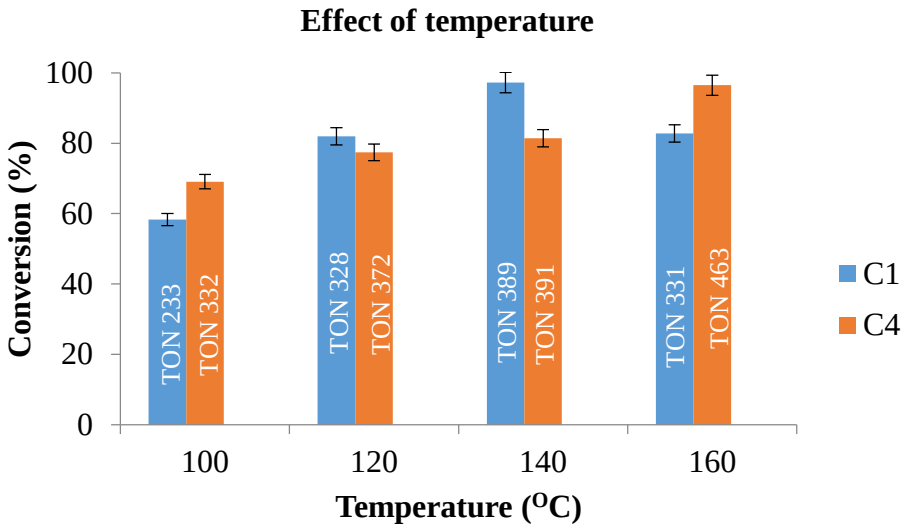

Figure S14. Effect of temperature in the hydrogenation of FF

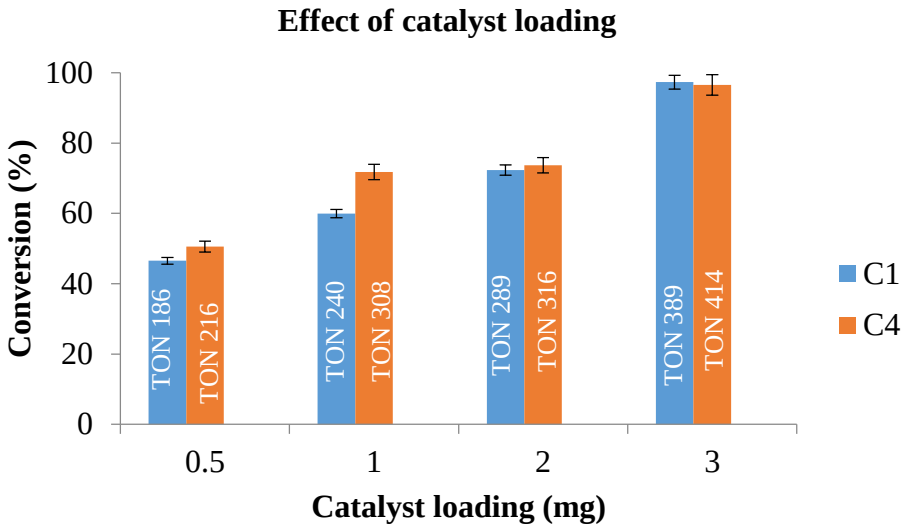

Figure S15. Effect of catalyst loading in the hydrogenation of FF

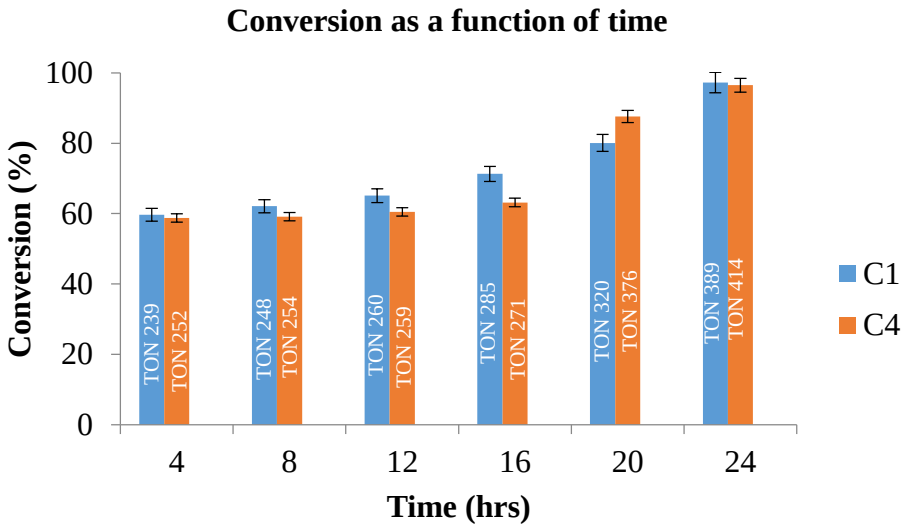

Figure S16. Effect of time in the hydrogenation of FF

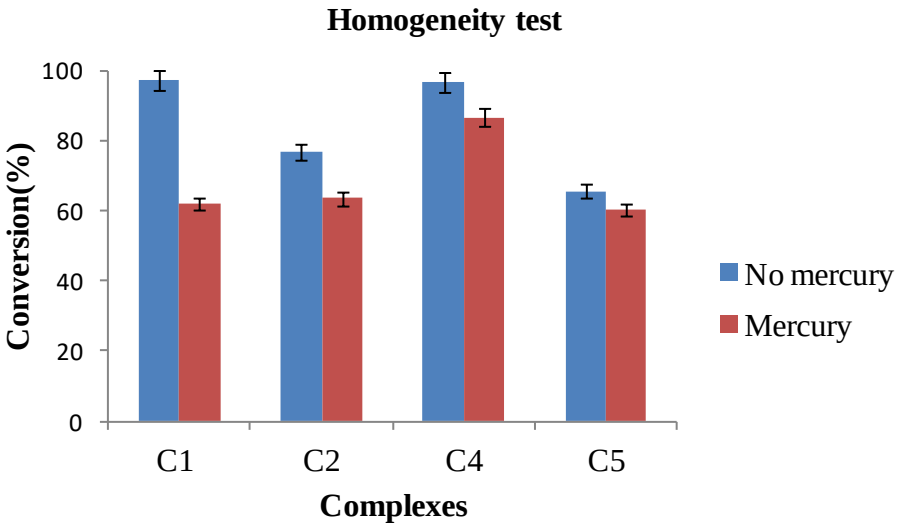

Figure S17. Homogeneity test during the hydrogenation of FF to FA using pre-catalysts (**C1, C2, C4, C5**)

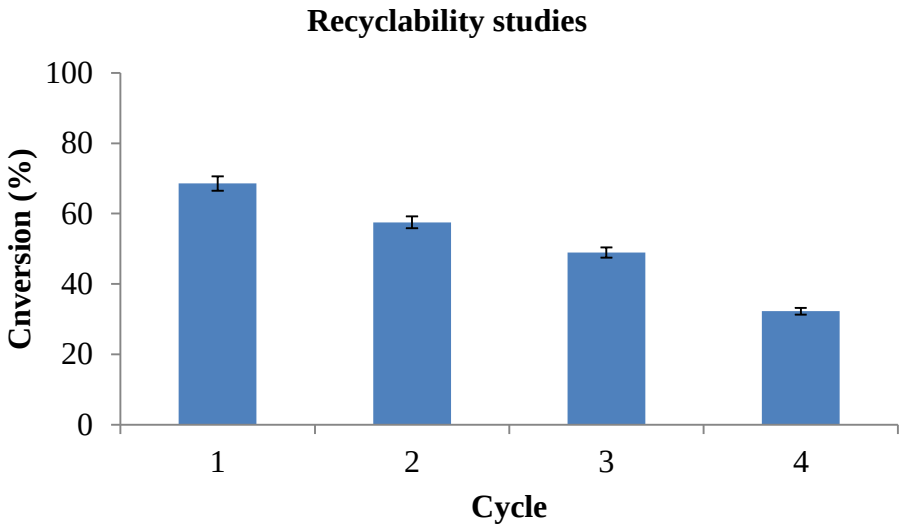

Figure S18. Recyclability of pre-catalyst **Si-1.**

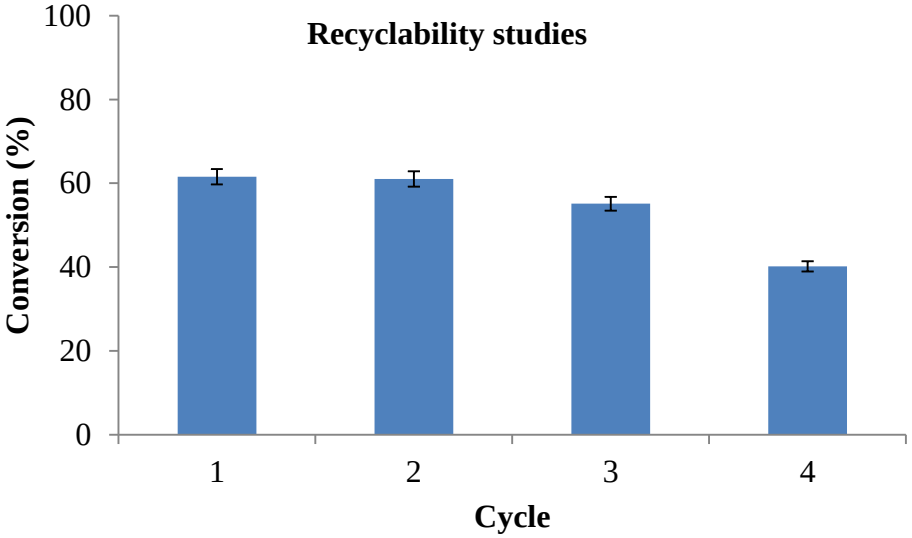

Figure S19. Recyclability of pre-catalyst **Si-2**.

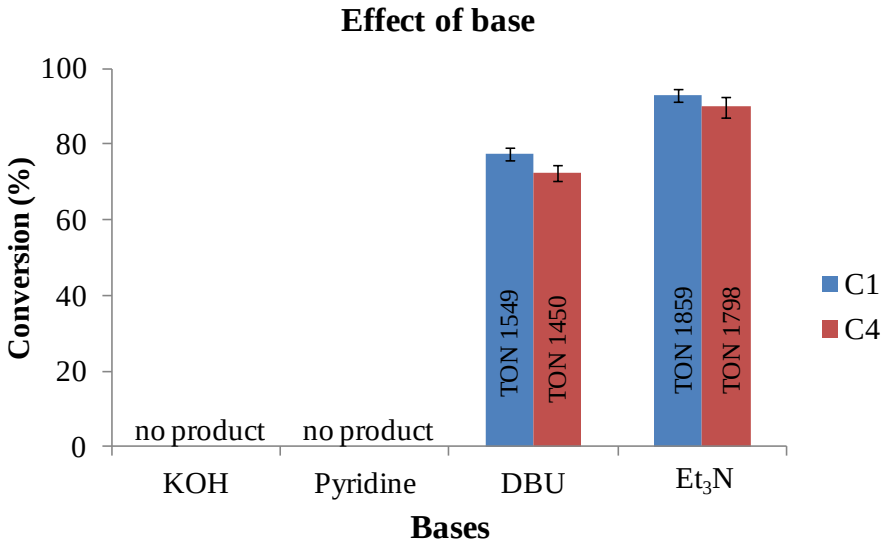

Figure S20. Effect of base in the catalytic transfer hydrogenation of FF

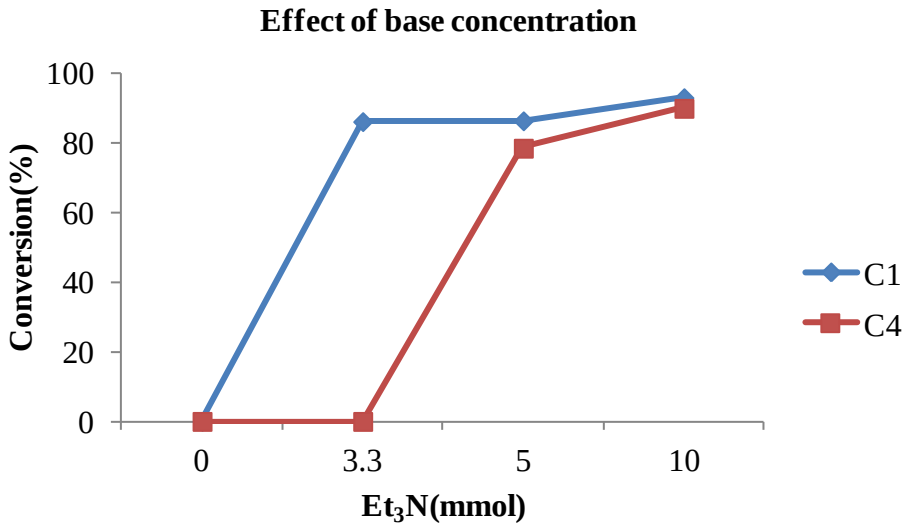

Figure S21. Effect of base concentration in the catalytic transfer hydrogenation of FF.

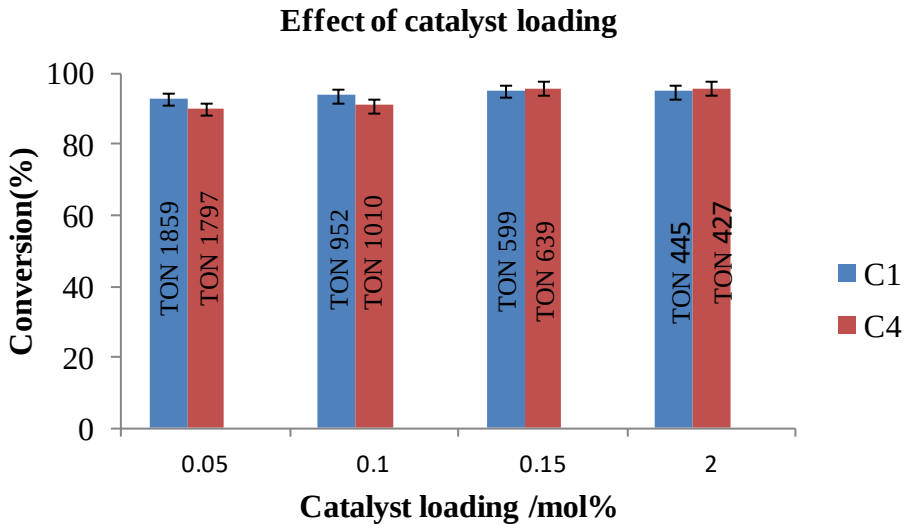

Figure S22. Effect of catalyst loading in the catalytic transfer hydrogenation of FF.

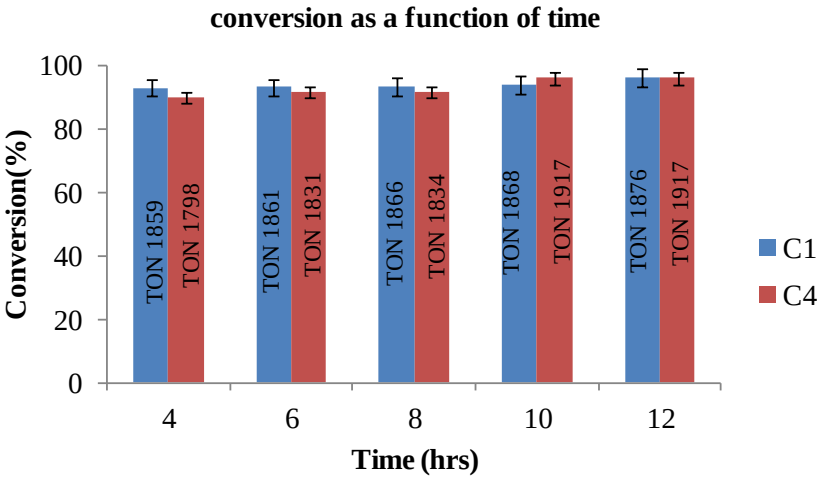

Figure S23. Conversion as a function of time in the catalytic transfer hydrogenation of FF

Table S2 Results of TON and TOF versus time obtained from catalytic transfer hydrogenation of FF

Entry	**Complex**	**Time/h**	**TON**	**TOF/h-^{1}**
1	**C1**	4	1859	465
2	**C4**	4	1798	450
3	**C1**	6	1861	310
4	**C4**	6	1831	305

5	**C1**	8	1866	233
6	**C4**	8	1834	229
7	**C1**	10	1868	187
8	**C4**	10	1917	192
9	**C1**	12	1876	156
10	**C4**	12	1917	159

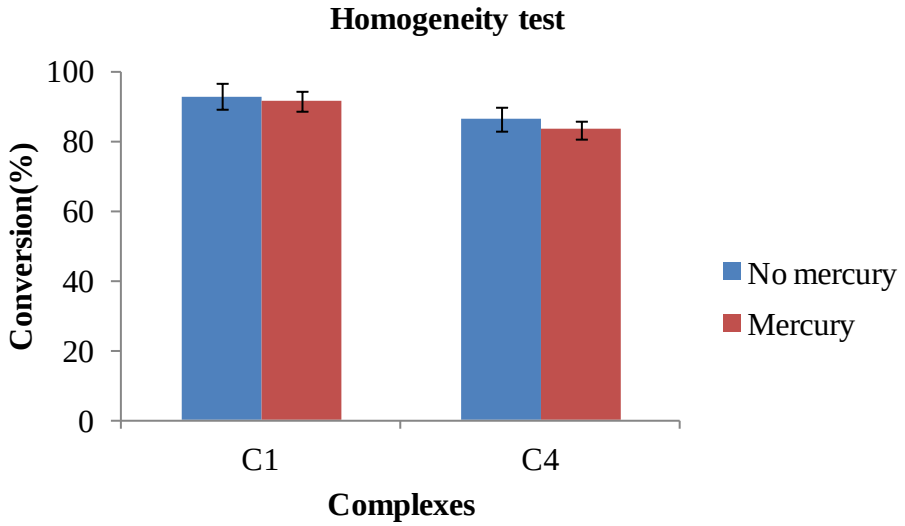

Figure S24. Homogeneity test in the catalytic transfer hydrogenation of FF using pre-catalysts **C1** and **C4.**

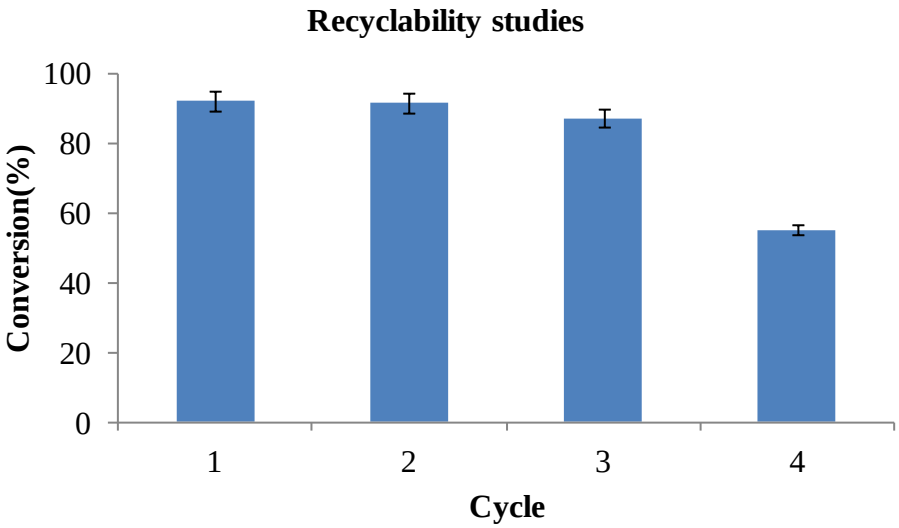

Figure S25. Recyclability of precatalyst **C1**

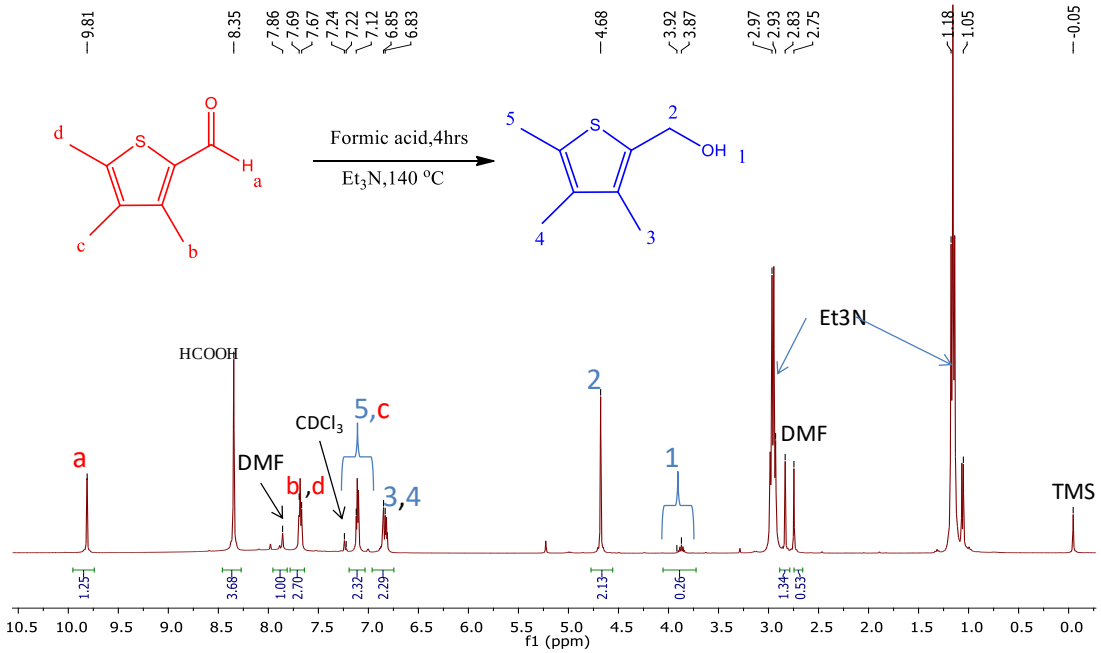

Figure S26. ^{1}H NMR spectrum of the transfer hydrogenation of 2-thiophenecarboxaldehyde to 2-thiophenemethanol using pre-catalyst **C1** in $CDCl_3$, DMF internal standard (500 MHz).